The Pennsylvania State University

The Graduate School

The Department of Anatomy

CENTRAL MECHANISMS OF EXPERIMENTAL TBI-INDUCED GASTROPARESIS

A Thesis in

Anatomy

by

Kristina R. Pugh

Submitted in Partial Fulfillment
of the Requirements
for the Degree of

Master of Science

May 2014

The thesis of Kristina R. Pugh was reviewed and approved* by the following:

Gregory M. Holmes

Associate Professor of Neural and Behavioral Sciences

Thesis Advisor

R. Alberto Travagli

Professor Neural & Behavioral Sciences

Patricia J. McLaughlin

Distinguished Professor Neural & Behavioral Sciences

Director Graduate Program in Anatomy

*Signatures are on file in the Graduate School

Abstract

Traumatic Brain Injury (TBI) in humans occurs as a result of acceleration and/or deceleration forces, blunt force impact, and penetrating wounds to the head. Individuals with TBI often present with a poor response to supplemental nutritional support while in intensive care and the mechanisms for this failure remain unknown. Our own preliminary data show that experimental TBI induces gastrointestinal (GI) dysmotility while other experimental models have demonstrated that TBI initiates a cascade of GI mucosal barrier pathologies, all of which are hypothesized to contribute to prolonged dysregulation of nutrient homeostasis. The control of gastric motility is dominated by vagal neurocircuitry and the vagal connection between higher brain regions and the GI tract, referred to as the brain-gut axis, is an important link in the modulation of GI function by homeostatic and emotional processes. It has been shown that TBI induces at least a brief upregulation of corticotropin-releasing factor (CRF) in the paraventricular nucleus (PVN) of the hypothalamus and the amygdala. Experimental models of stress-mediated gastric dysmotility have demonstrated the role of CRF in GI dysfunction. The central hypothesis of this thesis is that post-TBI upregulation of CRF plays a key role in the central mechanisms leading to post-TBI gastroparesis. In all experiments, male Wistar rats were used and injured via the fluid percussion model (FP-TBI). Outcomes were measured using a combination of immunohistochemical, molecular, physiological and non-invasive gastric emptying tests. Parameters of lesion severity were determined by peak pressure of the fluid percussion wave, righting time, and mortality rate. Analysis of these parameters revealed that experimental subjects segregated into three basic populations, mild-injury, moderate-injury and fatal-injury. In control rats, $t_{(max)}$ and $t_{1/2}$ measurements of gastric emptying were not significantly different from FP-TBI at any post-surgical time point. There was a non-significant trend for an elevation of

maximum cumulative dose at one week post injury (P=0.08). Immunohistochemical detection of CRF could not reliably be detected by the immunohistochemical protocol employed in this study. Microdissection of the PVN from control and FP-TBI rats yielded no significant differences in CRF mRNA expression between groups (P>0.05). Additionally, microinjection of oxytocin into the DVC of control, mild and moderate FP-TBI rats did not significantly alter gastric tone, although there was a non-significant trend toward a reversal of the effect of oxytocin in moderate FP-TBI. It was concluded from these present data that CRF is not robustly upregulated following the current FP-TBI parameters. The post-TBI mechanism leading to gastric dysfunction remains to be determined by further experimentation.

Table of Contents

List of Tables……vii

List of Figures……viii

Abbreviations……ix

Chapter 1: Introduction 1

1.1 Human Epidemiology and the Cost of Traumatic Brain Injury 1

1.2 Categories of TBI and Principle Deficits 1

1.3 Experimental Models of TBI 3

1.4 Vagal Regulation of Gastric Reflex Functions 5

1.5 Potential Mechanisms of TBI-induced Gastroparesis 6

1.6 Relevance of Rodent Experimental TBI Model 8

Chapter 2: Hypothesis and Specific Aims 9

2.1 Hypothesis 9

2.2 Specific Aim 1 9

2.3 Specific Aim 2 9

2.4 Specific Aim 3 10

Chapter 3: Methods 11

3.1 Animal Model 11

3.2 Surgical Procedures- TBI 11

3.3 $^{[13]}$C Breath Testing 14

3.4 Surgical Procedures- Strain Gauge Implantation and Recording of Gastric Motility 15

3.5 Tissue Harvesting Procedures 16

3.6 Immunohistochemistry 16

3.7 RNA Isolation, Reverse Transcription and q-PCR 17

3.7.1 RNA Isolation 17

3.7.2 Reverse Transcription and q-PCR 17

3.8 Statistical Analysis 18

Chapter 4: Results 19

4.1 Characteristics of the FP-TBI Model 19

4.2 Gastric Emptying Was Not Significantly Reduced by FP-TBI 20

4.3 Immunohistochemistry Failed to Detect the Expression of CRF in the PVN Following FP-TBI 23
4.4 CRF mRNA Is Not Upregulated in the PVN following FP-TBI 23
4.5 The Effect of Oxytocin on Gastric Motility in FP-TBI and Control Animals 24
Chapter 5: Discussion 27
Chapter 6: Conclusion 31
Chapter 7: Future Directions 32
References 33

List of Tables

Table 1: The total number of animal mortalities across all experiments.

Table 2: The number of animal mortalities in each specific aim.

Table 3: T_{max} and $T_{1/2}$ values for control and FP-TBI animals.

List of Figures

Figure 1: Pattern of hypothetical force distribution from midline FP-TBI.

Figure 2: Simplified schematic diagram of the gastric vago-vagal reflex circuit.

Figure 3: Diagram of craniotomy and placement of injury hub.

Figure 4: Photograph of FP-TBI device.

Figure 5: Overlays of three representative FP-TBI force traces.

Figure 6: Cumulative dose of ^{13}C respired.

Figure 7: CRF-immunolabeled tissue from Wistar rats.

Figure 8: Comparisons of CRF mRNA/β-actin ratios.

Figure 9: Representative raw motility trace.

Figure 10: Graphic summary of the change in gastric tone.

Abbreviations

A: Adenine

Ach: Acetylcholine

ANOV: Analysis of variance

AP: Area postrema

ATM: Atmosphere (of pressure)

BW: Body weight

C: Cytosine

cm: Centimeter

CNS: Central nervous system

CO_2: Carbon dioxide

CRF: Corticotropin-releasing factor

CSF: Cerebral spinal fluid

DMV: Dorsal motor nucleus of the vagus

dNTP: Deoxyribonucleotide triphosphate

DVC: Dorsal vagal complex

Fig: Figure

FPI: Fluid percussion injury

FP-TBI: Fluid percussion traumatic brain injury

g: Gram

G: Guanine

GABA: Gamma-Aminobutyric acid

GCS: Glascow, coma scale

GI: Gastrointestinal

IED: Improvised explosive devices

IHC: Immunohistochemistry

IRIS: Infra Red Isotope Analyser

JoVE: Journal of Visualized Experiments

kg: Kilograms

L: Liter

MEe: Median eminence

mg: Milligrams

ml: Milliliter

mRNA: Messenger Ribonucleic Acid

NDS: Normal donkey serum

NANC: Non-adrenergic, non-cholinergic

NO: Nitric oxide

NTS: Nucleus tractus solitarius

PBS: Phosphate-buffered saline

PVN: Paraventricular nucleus (of the hypothalamus)

Q-PCR: Real Time Polymerase Chain Reaction

RNA: Ribonucleic Acid

RT: Reverse transcriptase

RT-PCR: Reverse Transcriptase Polymerase Chain Reaction

SC: Standard concentration

SEM: Standard error of the mean

T: Thymine

TBI: Traumatic brain injury

µl: Microliter

Chapter 1: Introduction

1.1 Human Epidemiology and the Cost of Traumatic Brain Injury:

Traumatic Brain Injury (TBI) is a major medical issue in the United States, affecting more than 1.7 million people each year and often resulting in morbidity, cognitive impairment and mortality (CDC, 2014). More than 500,000 civilian deaths result from TBI and as many as 5.3 million individuals live with long-term disabilities in the United States alone (CDC, 2014). Among the leading causes of TBI in the United States are falls, motor vehicle crashes, blunt impact forces, and assaults (CDC, 2014). Furthermore, TBI has become ever more frequent in recent military engagements, showing involvement in more than 20% of all combat injuries (Rosario et al., 2012).

Healthcare costs associated with TBI exceed 60-75 billion dollars annually (Rosario et al., 2012 and CDC, 2014). Costs associated with long-term TBI continue beyond the initial injury. A controlled population-based study concluded that, over a 6 year period, TBI patients paid $4,906 more in healthcare than their healthy counterparts (Leibson et al., 2012). Military estimates for the cost of care for veterans with TBI-related co-morbidities are projected to exceed $50,000 per case by the year 2035 (Geiling et al., 2012).

1.2 Categories of TBI and Principal Deficits

The current classification of TBI in humans is regarded as forming a continuum ranging from concussion, mild brain injury, to catastrophic head trauma. TBI is most commonly categorized according to the Glascow, Coma Scale (GCS); (Teasdale & Jennett, 1974). The GCS is comprised of separate scores for motor, verbal and eye responses produced by external stimuli. A person's level of deficit is semi-quantitatively graded on a cumulative scale of 3-15 thereby

permitting classification ranging from mild (concussion, GCS 13-15), moderate (GCS 9-12) to severe (GCS 3-8); (Bruns & Hauser, 2003).

Open-head TBI occurs as a result of an object, such as projectile, of force capable of penetrating the skull, dura and brain matter. The more common closed-head TBI occurs as a result of high impact acceleration and/ or deceleration forces to the head as often seen in automobile accidents, falls, sports injuries and violence. The resulting coup contrecoup injury causes the brain to move violently inside the skull, possibly striking the cranial walls, and produces vascular hemorrhage as well as neural shearing forces that result in diffuse axonal damage throughout the brain (Gaetz, 2004). A patient with only a mild form of TBI may experience a loss of consciousness for a few seconds or minutes, headache, dizziness, confusion, blurred vision and trouble with memory, concentration or attention (Walker & Tesco, 2013). In addition to these symptoms, a patient with a moderate to severe TBI may experience nausea and vomiting, slurred speech, numbness in the extremities, loss of coordination, and convulsions or seizures (Pilitsis & Rengachary, 2001).

In addition to the cognitive and emotional derangements that occur following TBI, remote tissue injury and dysfunction commonly occur (Catania et al., 2009). Increases in muscle wasting, energy expenditure, and catabolism are also seen in patients with moderate to severe TBI (Krakau et al., 2006). Recent reports have indicated long-term impairments in the nutritional state of the TBI patient, including over 68% of patients exhibiting signs of malnourishment 6 months (Krakau et al., 2007) to 10 years post-injury (Horneman et al., 2005.) Malnutrition is furthermore problematic in that low body weight increases the risk of developing infection and prolongs the recovery process from TBI. Nutrient homeostasis and support are associated with favorable patient outcome. For TBI patients, clinical data suggest that a parenteral route is

superior to enteral supplementation, though parenteral supplementation is associated with shortcomings (Wang et al., 2013). These findings underscore the need for developing both alternative nutritional strategies to help improve the specific nutritional requirements of TBI patients (Moinard et al., 2012) as well as a mechanistic understanding of the cause of post-TBI GI dysfunction.

1.3 Experimental Models of TBI:

Clinically relevant models of experimental TBI have been developed to mimic the mechanical impact to brain tissue as seen in human injury (reviewed in Xiong et al., 2013). Fluid percussion injury (FPI) was initially designed to generate coup-countrecoup injury in an animal model and results in a mixed model of focal and diffuse-injury TBI (Thompson et al., 2005). Other models induce TBI through use of a weight drop to the skull surface (Foda & Marmarou, 1994) or controlled cortical impact with a piston-actuated impactor (Dixon et al., 1991). Recently a rat model of angular acceleration TBI has been presented (Ellingson et al., 2005). While no model of experimentally induced TBI fully encompasses the complexities of human head injury, the FPI model has been shown to result in more diffuse injury than the weight drop model (Clausen & Hillered, 2005). Specifically, FPI affects a greater proportion of contralateral tissue, and produces neural degeneration in deeper brain regions including the brainstem long fiber tracts (Hallam et al., 2004) and thus is the model proposed for these experiments.

In FP-TBI, the experimental injury may be directed laterally or along the midline. A midline injury location induces a diffuse injury with bilateral damage whereas a lateral injury location induces a focal injury with a diffuse component (Lifshitz et al., 2009). Furthermore, the bilateral effects produced by a midline injury models an injury that is most closely related to

human TBI caused by automobile accidents or sports injuries. This model replicates the neuropathology of human brain injury and produces an expected 20% mortality due to pulmonary edema and apnea. This is a normal and desired outcome of TBI animal models because it accurately portrays human TBI (Lifshitz et al., 2009). In the rat model, some of these symptoms can be directly observed as well as hemorrhage or herniation at the site of the injury and apnea.

During FP-TBI, the fluid wave hits the brain and the injury diffuses out from the point of contact, affecting a very large area of the brain, as far rostral as the olfactory bulbs (Fig. 1). In other models, a focal injury results that merely affects one small area of the brain, similar to the effects of a pin-prick or a knife-stab. During motor-vehicle accidents, sports injuries, or concussive forces of the blast waves from improvised explosive devices (IED's) humans will receive injuries that will more closely resemble FP-TBI results as opposed to the other methods of injury. Neither the weight-drop nor the controlled cortical impact model inflicts a diffuse axonal injury like FP-TBI, only a focal injury. In addition, both of these alternative models have more possible complications and limitations including skull fracture, difficulty placing the intubation tube, and higher mortality rates (Lifshitz et al., 2009).

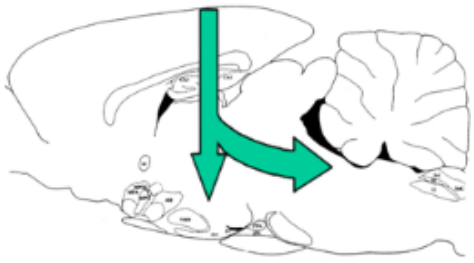

Figure 1. Pattern of hypothetical force distribution from midline FP-TBI. The injury diffuses out from the point of contact, affecting a very large area of the brain.

1.4 Vagal Regulation of Gastric Reflex Functions:

Clinicians and scientists have long recognized the cognitive and emotional deficits that arise as a result of TBI while more recent reports recognize that TBI induces both gastrointestinal (GI) dysmotility and an imbalance of GI and nutrient homeostasis. This relationship between the brain and GI function forms the basis for the brain-gut axis. Arguably a central link in the brain-gut axis is the neural modulation of digestive reflexes via the vagus nerve. Afferent fibers within the vagus nerve, whose cell bodies are located in the jugular and nodose ganglia, relay chemical and/or mechanical stimuli from the thoracic and visceral organs to the brainstem by way of the tractus solitarius (Fig. 2); (reviewed in Travagli, 2006). These fibers terminate as a glutamatergic synapse on neurons within the nucleus tractus solitarius (NTS). These second-order NTS neurons synapse on gastric projecting dorsal motor nucleus of the vagus (DMV) neurons through a GABAergic, glutamatergic, or noradrenergic synapse. The inhibitory neurotransmitter GABA is the most important regulator of basal gastric function (Babic et al., 2011). Within the brainstem, the medullary dorsal vagal complex (DVC) consists of the area postrema (AP), NTS and the DMV. The DVC integrates visceral afferent input from higher sources within the CNS and provides parasympathetic motor efferents to the GI tract thereby regulating gastric compliance, motility, as well as esophageal and pyloric sphincter tone. The DMV efferents project to the stomach or intestine where the synapse on the post-ganglionic enteric neurons on the organ itself. These efferents are composed of an inhibitory pathway, [nonadrenergic, non-cholinergic, (NANC) pathway which uses nitric oxide (NO) or vasoactive intestinal polypeptide as a neurotransmitter] and an excitatory pathway, which uses acetylcholine (Ach) as a neurotransmitter. As a result, the DVC influences GI functions important for the relaying of digested food particles from the stomach to the small intestine. For example, vagal

denervation to the stomach slows the rate of gastric emptying of solids through decreased gastric motility and reduced gastric compliance.

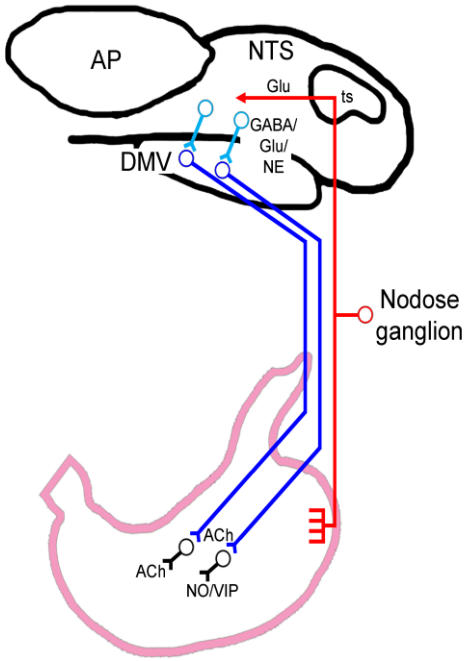

Figure 2. Simplified schematic diagram of the gastric vago-vagal reflex circuit. The vagal afferents synapse in the NTS (glutamatergic). These second-order NTS neurons synapse on gastric projecting DMV neurons (GABAergic, glutamatergic, or noradrenergic). The DMV efferents project to the stomach or intestine where they synapse on the post-ganglionic enteric neurons on the organ.

1.5 Potential Mechanisms of TBI-induced Gastroparesis:

Experimental TBI has been found to cause increased gut-permeability which can lead to complications such as bacterial translocation, (Hang et al., 2003; Bansal et al., 2009) inflammation, (Hang et al., 2003; Wang et al., 2011) and even multi-system organ failure (Coskun et al., 1997). One of the major systems commonly affected by TBI is the visual system including the optic nerve and the optic chiasm. Reactive axonal changes including swelling and deterioration were observed as a result of the forces seen in TBI (Cheng & Povlishock, 1988). The optic nerve was found to have post-TBI axonal swelling and disconnection (Wang et al., 2011).

This damage to the optic nerve and tract suggests that the adjacent hypothalamus and pituitary are also vulnerable to TBI as well. The multi-organ functional impairments that result

from TBI could be partially caused by hypothalamic-pituitary dysfunction. The unique and fragile anatomy of the hypothalamic-pituitary stalk can be easily damaged from shearing forces along the base of the skull. Patients with post-TBI hypopituitarism often present as overweight rather than malnourished (Ulfrasson et al., 2013).

Increasingly complex levels of neural integration and physiological response of the organism to homeostatic challenges (stress) are being recognized (Ulrich-Lai & Herman, 2009). Conflicting results from previous studies present effects of TBI as eliciting a heightened stress response in the first weeks after TBI (Griesbach et al., 2011) or reduced response (Taylor et al., 2008). Corticosterone, a hormone produced by the adrenal glands that plays a role in the stress response, was found to be elevated which has been demonstrated to negatively affect emotional health and the plasticity of the hippocampus (Griesbach et al., 2011). Stress has been shown to have negative effects on neural plasticity and it is likely that increases in corticosterone after TBI may also inhibit neuroplasticity, though the full extent of this diminished neuroplasticity remains unknown (Griesbach et al., 2011). Briefly, corticotropin-releasing factor (CRF) is a peptide hormone and neurotransmitter produced by parvocellular neuroendocrine cells within the paraventricular nucleus (PVN) of the hypothalamus and is released at the median eminence from neurosecretory terminals of these parvocellular neurons where it then gets transported to the anterior pituitary to signal the release of adrenocorticotropic hormone and β-endorphin which are involved in the stress response. CRF is synthesized centrally within the PVN and contributes largely to proper autonomic functioning. CRF is released during emotional stress (Zheng et al., 2010) or following trauma such as TBI (Roe et al., 1998) and is known to induce gastric inhibition through a vagally-dependent mechanism (Lewis et al., 2002). CRF inhibits vagal nerve activity through activation of the inhibitory limb of the DMV (Lewis et al., 2002).

Oxytocin may also play a role in post-TBI gastroparesis by counteracting the effects of CRF. In a model of resistant stress, oxytocin is known to have anti-stress effects and modulate the regulation of the stress response (Babygirija et al., 2012). The PVN, as well as other hypothalamic nuclei, contains oxytocin-secreting neurons and oxytocin production is diminished as protein synthesis is downregulated following TBI (Petrov et. al., 2001). In other induced stress models, oxytocin levels are increased and oxytocin works as an anti-stress agent by attenuating CRF signaling specifically with regard to the restoration of stress-induced, gastric dysmotility (Zheng et al., 2010). In the case of TBI, however, gastric dysfunction remains persistent in TBI models, which suggests that TBI may decrease hypothalamic oxytocin signaling to the NTS.

1.6 Relevance of Rodent Experimental TBI Model

Recent advances by the TBI research community has fostered a clearer understanding of the interrelated cellular and biochemical processes which comprise TBI, identified the challenges for successful sparing or regeneration of damaged tissue, and expended considerable intellectual capital upon that recovery of cognitive function after TBI. The present work is ground-breaking because there is currently no understanding of the mechanisms responsible for TBI-induced gastric dysmotility. It is known that TBI causes gastric dysmotility and it is known that TBI causes an upregulation of CRF, but the connection between these two conclusions has not been discovered. By learning how CRF and related peptides take over the brain-gut axis following neuronal damage, we will better understand how to develop therapeutic strategies to restore normal gastric functioning. Using the results of research like that being done in the present study, strategies must be developed in order to limit brain damage due to TBI and to improve long-term recovery of function for patients with TBI.

Chapter 2: Hypothesis and Specific Aims

2.1 Hypothesis

Based upon preliminary data and review of the literature, this thesis put forward the following novel, overarching hypothesis: Experimental traumatic brain injury provokes gastric dysmotility through an upregulation of CRF within the hypothalamic PVN. In turn, CRF ultimately induces an inhibition of gastric projecting neurons within the dorsal vagal complex.

2.2. Specific Aim 1

The ^{13}C-octanoic acid breath test is a validated, non-invasive, means of indirectly measuring gastric emptying in humans and animals (Schoonjans et al., 2002). These experiments will be conducted in awake, freely behaving, FP-TBI and surgical control rats. We hypothesize that gastric emptying in experimental FP-TBI rats is significantly delayed in comparison to control animals. Delay of gastric emptying will be defined as an increase in the time to reach maximum respired $^{13}CO_2$ (T_{max}) following feeding as well as the time to empty one-half of the gastric contents ($T_{1/2}$) as calculated by the analysis of the cumulative percentage of respired $^{13}CO_2$. Rats will be tested pre-operatively and at three days, one week, and three weeks following FP-TBI or control surgery. This time course was chosen in order to detect the magnitude and duration of delayed gastric emptying.

2.3 Specific Aim 2

It has been shown that TBI induces an upregulation of CRF within the hypothalamic PVN. Elevated levels of endogenous CRF and exogenously administered CRF are well recognized to induce dysmotility of the upper GI tract. We hypothesize that rats receiving our model of FP-TBI will also express greater levels of CRF in the PVN. In order to detect and

localize neuronal CRF in CNS nuclei of experimental vs. control animals, free-floating IHC will initially be used to detect CRF upregulation in the PVN of the hypothalamus. Paraformaldehyde-fixed tissue samples will be cut 40μm on a freezing stage microtome and processed using a standard IHC protocol. In order to quantify the increase of CRF following FP-TBI, RNA will be extracted from PVN micropunches from control and FP-TBI groups, and analyzed using RT-PCR and Q-PCR protocols to detect mRNA levels of CRF. Rats will be tested at 1 day, 3 days and 1 week following FP-TBI or control surgery.

2.4 Specific Aim 3

Preliminary data suggests that gastric contractions are diminished at least 3 days following experimental FP-TBI. In addition, other unpublished studies have demonstrated that CRF pretreatment of the dorsal medulla provokes a reversal of the gastroinhibitory effect of oxytocin microinjected into the DVC. To measure the extent of gastric contractions occurring in experimental vs. control animals using strain gauges sutured to the gastric surface and to assess the effects of oxytocin injected into the area postrema of the brainstem. Strain gauges of our own design (Holmes et. al., JoVE, in press) were used to detect smooth muscle contractions in animals from both control and experimental groups. The brainstem will then be exposed and a glass micropipette will be lowered into the left dorsal vagal complex (DVC). Microinjection of oxytocin will be made to test for an anticipated, post-FP-TBI, shift in the vagally-mediated gastric motility or tone. Rats will be tested at 3 days and 1 week following FP-TBI or control surgery.

Chapter 3: Methods

3.1 Animal Model

All experiments used equal groups of experimental and control male Wistar rats. Rats were approximately eight weeks of age upon entrance into the experiment and were housed in litters of four in a room maintained at 21-24ºC on a 12:12-hour light-dark cycle and food and water *ad libitum*. After surgery, animals were housed singly and observed daily. All procedures were performed according to National Institutes of Health guidelines and were approved by the Institutional Animal Care and Use Committee at the Penn State University College of Medicine.

3.2 Surgical Procedures- TBI

All recovery surgical procedures utilized aseptic technique, male rats were deeply anesthetized with isoflurane (3-5% concentration), administered pre-operative buprenorphine (0.01mg/kg SC) as an analgesic, and enrofloxacin (Baytril, 2.5 mg/kg SC) as an antibiotic. Surgical sites were shaved and scrubbed with Nolvasan and 95% ethanol. During all surgical procedures, anesthetized rats were maintained at 37±1 °C using a feedback-controlled warming pad. To ensure proper depth of anesthesia, reflex withdrawal in response to toe-pinch was tested. Post-operatively, animals were administered 5 ml of warmed lactated Ringers and placed in a warm incubator until ambulatory. Post-operative analgesics (buprenorphine; 0.01mg/kg SC bid) were administered for two days.

FP-TBI was performed using the using the device designed byVirginia Commonwealth University (Dixon et al., 1987). Once the animal was in a deep anesthetic plane, a craniotomy was performed between Bregma and Lambda centered on the sagittal suture in order to expose the dural surface (Fig. 3). Following a midline incision of the scalp, a 4.7 mm diameter trephine

was used to produce the midline craniotomy. The bone was removed taking care not to disturb the underlying dura and sagittal sinus. If the superior sagittal sinus was perforated, the animal was immediately removed from the study since profuse bleeding and death often occurred. An injury hub was fabricated from a luer-lock hypodermic needle. The tip of the needle, along with some of the colored plastic tip (the future hub) was removed using a scalpel blade. The proximal part of the hub was saved and beveled so that the diameter of the hole was exactly 4.7 mm and securely interfaced within the trephination. The injury hub was then cemented into place over the exposed area using dental acrylic and the animal was allowed to recover from anesthesia.

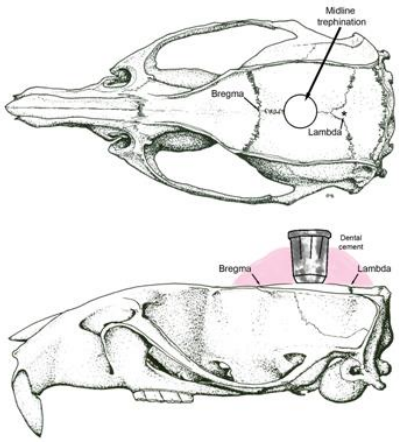

Figure 3. Schematic diagram of craniotomy location and placement of injury hub. The craniotomy is performed between Bregma and Lambda centered over the median sagittal sinus and an injury hub is secured over the craniotomy.

At least 90 minutes after recovering from the initial isoflurane anesthesia, the rat was lightly re-anesthetized with isoflurane and the saline-filled injury hub was fitted onto the fluid percussion injury device (Custom Design and Fabrication South LLC, Petersburg, VA) so that the exposed brain tissue was in direct contact with the water-filled cylinder that generates the impact (Lifshitz et al., 2009). FP-TBI employs a swinging pendulum that strikes a fluid-filled cylinder (Fig. 4). A highly consistent pressure wave was created inside of the cylinder that was then transmitted through the water onto the exposed brain of the rat. Using the device, a 1.22 atmosphere displacement of the midline dura was administered. The impact was administered

once a normal breathing pattern resumed (1-2 breaths/second) and before sensitivity to foot pinch stimulation occurred. Immediately after the injury, the injury hub was gently removed en bloc by applying pressure to the bridge of the nose while the hub remained attached to the device. The occurrence of apnea, seizure, brain herniation and hemorrhage was visually noted. Animals displaying apnea were manually resuscitated by thoracic compression. Animals displaying seizures lasting longer than one minute were removed from the study and euthanized. If the dura was compromised (brain herniation or hemorrhage) the animal was removed from the study and euthanized. Following inspection, the animal was placed in a supine position and the time to spontaneous righting reflex was recorded. Following the determination of the righting reflex, the rat was lightly re-anesthetized and the scalp was sutured with 4-0 nylon suture, and the rat was allowed to recover from isoflurane before being housed. Control rats were given a craniotomy, attached to the FP-TBI device, removed from the device before TBI was given, sutured with nylon sutures, and allowed to recover from isoflurane before being housed. Post-operative pain was alleviated with buprenorphine (0.01 mg/kg BW SC) as necessary. All rats were monitored for one day, three days, one week, or three weeks and then perfused for anatomical or histochemical analysis.

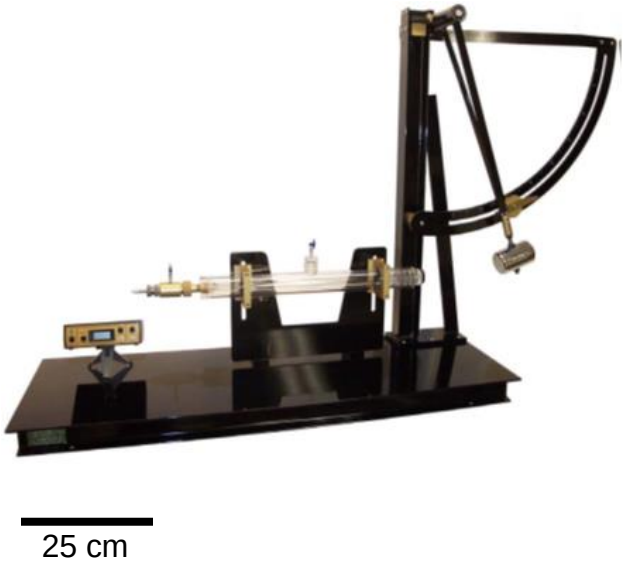

Figure 4. Photograph of FP-TBI device manufactured by Custom Design and Fabrication. The injury hub is connected to the FP-TBI device which consists of a falling pendulum that strikes a fluid-filled cylinder. A highly consistent pressure wave is created inside of the cylinder that is transmitted through the water onto the exposed brain tissue.

3.3 $^{[13]}$C Breath Testing

Rats (both FP-TBI (n=12) and surgical control (n=11) were food deprived for at least 16 hours before experimentation. Rats were placed in a 3 L airtight Plexiglas container with an inlet and outlet valve. Room air was circulated through the chamber at a rate that held CO_2 levels between 0.3-0.6%. Rats were given a substrate of a solid meal consisting of a 1 g pancake (commercial pancake mix) containing a 2.0 mg dose of ^{13}C-tagged substrate (octanoic acid, 99% enrichment, Cambridge Isotope Laboratories, Andover, Massachusetts) that was freely consumed by the animal and the animal was monitored for six hours. For the first 70 minutes, 50 ml of air was automatically aspirated from the chamber at 5 minute intervals by the Wagner IRIS analyzer. Afterwards, samples were automatically collected at 15 minute intervals. Using the change in $^{13}CO_2$ level over baseline for each air sample, the maximum concentration (C_{max}; ‰) time to reach the maximum concentration in fractional dose/hour (T_{max}) and the gastric half emptying time ($T_{1/2}$) were calculated by the IRIS software. At the conclusion of the breath test,

animals were returned to their home cage. Rats were tested pre-operatively and at 3 days, 1 week and 3 week following FP-TBI or control surgery.

3.4 Surgical Procedures- Strain Gauge Implantation and Recording of Gastric Motility

Inactin anesthetized animals, after 16 hour food deprivation, were fitted with a tracheal cannula. A ventral laparotomy was performed to expose the stomach for instrumentation. Strain gauges of our own design (Holmes et. al., JoVE, in press) were sutured to the serosal surface on the anterior gastric corpus of experimental and control animals to detect smooth muscle contractions. The strain gauge was aligned perpendicular to the greater curvature in order to maximally detect circular smooth muscle contractions and attached to the distal stomach by 4-0 suture to record motility. The stomach was returned to the original anatomical position, the abdomen was infused with warmed, sterile saline. Once in place, the strain gage lead was exteriorized through the inferior portion of the abdominal laparotomy and the abdomen was closed in reverse layers. The signal was amplified via Quanta Metrics EXP CLSG-2 and recorded through the use of a polygraph chart recorder (model 79, Grass Instruments, Quincy, Massachusetts) and Datawave software (DataWave Technologies, Loveland, Colorado).

Rats were placed in a stereotaxic frame (Kopf Instruments, Tujunga, California) with the head at a -20 mm angle and a 2 cm midline incision was made over the occipital region. Skin and muscles were retracted, and the brainstem was exposed by gently dissecting the dura and arachnoid membranes. A glass micropipette (World Precision Instruments, Sarasota, Florida) that had been pulled to a diameter of 50 µm (model PE-2, Narishige, Japan) was lowered into the left dorsal vagal complex (DVC) with a micropositioner according to stereotaxic coordinates (0.1-0.3 mm rostral to calamus scriptorius, 0.1-0.2 mm mediolateral and 0.3 mm dorsoventral to

the surface of the medulla). Microinjection of PBS vehicle or oxytocin (100 pmol) was made to test for an anticipated, post-FP-TBI, dose response shift in the vagally-mediated gastric motility or tone.

3.5 Tissue Harvesting Procedures

For fresh CNS tissue, animals were decapitated using a small rodent guillotine (World Precision Instruments). Fresh CNS tissue was removed, wrapped in aluminum foil and immediately submerged in liquid nitrogen. Samples were then stored in -80°C. After freezing, samples were blocked to punch for the PVN and transferred to dry ice and then 40 mM tissue samples were cut on a freezing stage microtome.

For fixed CNS tissue, a transcardial perfusion was performed on all animals. A line is inserted into the left ventricle and the right atrium is cut to allow the outflow of blood. First PBS is pumped into the heart until all of the blood is drained. 4% paraformaldehyde is then pumped into the heart until the body becomes thoroughly fixed. Fixed CNS tissue is removed and stored in a 20% sucrose/ (4%) paraformaldehyde solution at 4ºC.

3.6 Immunohistochemistry (IHC)

Free-floating IHC was used to visualize the distribution and localization of CRF in the PVN of the hypothalamus. 40 μm tissue samples were cut on a freezing stage microtome and placed in PBS. A blocking solution of 10% Normal Donkey Serum (NDS) which consists of NDS, PBS and triton, (a detergent that solubilizes the tissue) was applied to the tissue samples for 1.5 to 2 hours. The blocking serum was removed and then, a primary antibody used for detecting CRF (Santa Cruz Biotechnology) was applied to the tissue sample for a minimum of 18 hours. A series of 3 10-minute PBS washes was performed and then followed with the secondary

antibody consisting of Biotinylated Donkey anti Goat IgG mixed with PBS. Tissue samples were incubated for 1.5 to 2 hours and followed by another series of 3 10-minute PBS washes. An Avidin-Biotin Complex Solution, (specifically the Vectastain Elite ABC kit, Vector Labs) was applied to the tissue samples for 1 hour and followed by another series of 3 10-minute PBS washes. The tissue samples were then incubated using the Vector SG kit as chromogen in a time critical reaction that took place over the course of 3-10 minutes. As soon as the tissue samples started to stain, they were washed with PBS in a series of 3 10-minute washes. The tissue samples were then mounted onto subbed/gel coated glass slides and allowed to dry overnight. Then next day the slides were cleared in Clear Rite and coverslipped with Permount for viewing.

3.7 RNA Isolation, Reverse Transcription Reaction and q-PCR

3.7.1 RNA Isolation

Whole brains that were blocked to isolate the PVN were maintained on dry ice and transferred to the frozen stage of the microtome. The rostral end of the brain was sectioned and then the brain was flipped and the caudal end of the brain was sectioned. Using a tissue punching tool, bilateral samples targeting the PVN were obtained and pooled for RNA Isolation.

3.7.2 Reverse Transcription and q-PCR

RNA was isolated using TRIzol (Invitrogen, Carlsbad, California) and RNeasy Microkit procedures (Qiagen, Valencia, California). Briefly, frozen tissue was homogenized in TRIzol using a glass homogenizer and Teflon pestle on ice, chloroform was added to lysate, and the mixture was centrifuged in microcentrifuge tubes to separate RNA. Ethanol was added to the upper aqueous phase, the mixture was applied to a RNeasy spin column and filtered by centrifugation. After several washes, the samples were subjected to an elution step using RNase-free water. Reverse transcription (RT) was conducted using the High Capacity cDNA Reverse

Transcription Kit (Applied Biosystems, Foster City, CA). For RT, ~1 μg of RNA from each sample was added to random primers (10×), dNTP (25×), MultiScribe reverse transcriptase (50 units/μl), RT buffer (10×) and RNase Inhibitor (20 units/μl) and incubated in a thermal cycler (Techne TC-412, Barloworld Scientific, Burlington, New Jersey) for 10 minutes at 25°C, then for 120 minutes at 37° C. Primers for β-actin were a QuantiTect Primer Assay (Qiagen). Primers for CRF were designed using Primer Express (Applied Biosystems). The following primers were used for CRF:

forward 5′-CCAGGGCAGAGCAGTTAGCT-3′

reverse 5′-GCAACATTTCATTTCCCGATAATC-3′

For real-time PCR, SYBR Green 2× Master Mix (Qiagen), forward and reverse primers (100 μM), and RT product (1μl of a 1:16 dilution) were added to a 384-well plate. The cycling parameters consisted of an initial 2 minute incubation at 50°C, followed by 10 minutes at 95°C, then 15 s at 95 °C, a 30 sec annealing step at 55°C and a 30 sec extension step at 72°C (55 cycles). A dissociation step (15 s at 95°C) was added following 55 cycles to determine specificity of primers. In this assay, the dissociation step confirmed the absence of nonspecific amplifications. Quantity of CRF mRNA was based on a standard curve and normalized to β-actin mRNA (ABI QuantStudio 12KFlex with available OpenArray block, Applied Biosystems).

3.8 Statistical Analysis

All results are expressed as mean ± SEM. Data analysis was completed using ANOV and post hoc comparisons and was analyzed by comparing values for each time point to sham animal values (Sigmaplot, Systat Software, Inc. San Jose, California). In all analyses, significance was assumed when $P<0.05$.

Chapter 4: Results

4.1 Characteristics of the FP-TBI Model

The mortality rate for the FP-TBI animals used across all specific aims was 20.00%. As seen in Table 1, there were 60 total animals prepared for FP-TBI, out of which there were 48 survivors and 12 mortalities.

Table 1. The total number of animal mortalities across all experiments.

Total	Survivors	Mortalities	Mortality %
60	48	12	20.00%

The mortality percentage for each specific aim is shown in Table 2. The mortality percentage for the ^{13}C-octanoic acid breath test was calculated to be 29.41%, the mortality percentage for the oxytocin microinjections into the brainstem was calculated to be 8.00% and the mortality percentage for the CRF localization was calculated to be 27.78%.

Table 2. The number of animal mortalities in each specific aim.

Specific Aim	Survivors	Mortalities	Mortality%
1	12	5	29.41%
2	13	5	27.78%
3	23	2	8.00%

Mild FP-TBIs (Fig. 5A) were characterized by righting reflex times of 5 minutes or less, moderate FP-TBIs (Fig. 5B) were characterized by righting reflex times of 8-20+ minutes, and

fatal FP-TBIs (Fig. 5C) were characterized by a mortality due to respiratory failure, breach of the dura which resulted in cerebral spinal fluid (CSF) leakage out of the nostrils or sagittal sinus hemorrhage. The mean righting time for all FP-TBI animals was 8:28 and the values ranged from 0:47- 22:25.

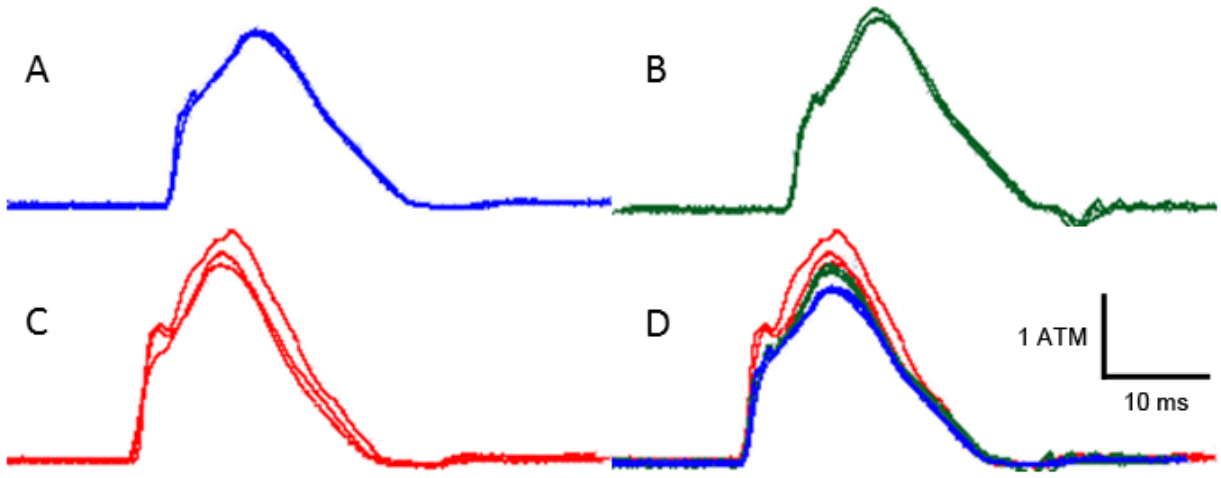

Figure 5. Overlays of three representative FP-TBI force traces from (A) mild; (B) moderate; or (C) fatal FP-TBIs that resulted in subject mortality. (D) The nine representative traces demonstrate the narrow range of pressure-wave differences in each outcome. The pendulum striking the piston on the fluid-filled cylinder is demarcated by the immediate rise in pressure on the force traces. The pressure is measured in atmospheres (ATM).

4.2 ^{13}C Gastric Emptying Was Not Significantly Reduced by FP-TBI

In conscious male Wistar rats (n=23) baseline values for T_{max} and $T_{1/2}$ were not statistically different in control (n=11) vs. FP-TBI (n=12) groups (data not shown). As seen in Table 3, values for T_{max} and $T_{1/2}$ were not statistically different in control vs. FP-TBI groups at 3 days, 1 week or 3 weeks ($P>0.05$).

Table 3. T_{max} and $T_{1/2}$ values for control and FP-TBI animals at 3 days, 1 week and 3 weeks.

	3 days		1 week		3 weeks	
	Control	FP-TBI	Control	FP-TBI	Control	FP-TBI
T_{max}	79.18±11.36	74±7.7	87.54±7.27	88.32±9.92	97.27±13.16	98.19±13.3
$T_{1/2}$	138.63±34.24	112.5±14.38	119±6.39	113.07±8.62	121.64±16.27	135.44±15.53

The cumulative dose of ^{13}C respired by control and sham animals for three days, one week, and three weeks post-FP-TBI or control surgery, there was no significance between the two groups. Qualitatively, the cumulative dose of the FP-TBI group was consistently higher than the control group at all three time periods (Fig. 6). However, the C_{max} at 350 minutes was not significantly different between FP-TBI and control ($P>0.05$).

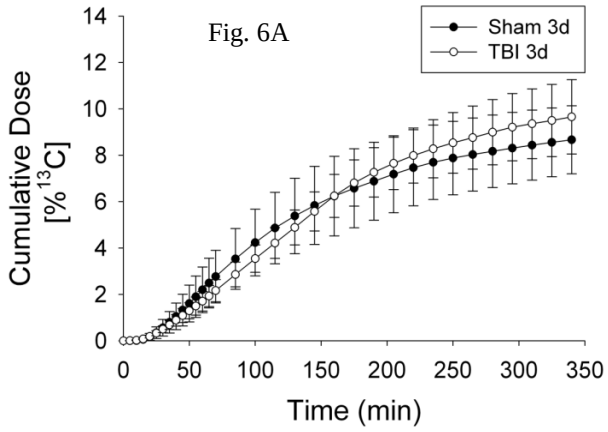

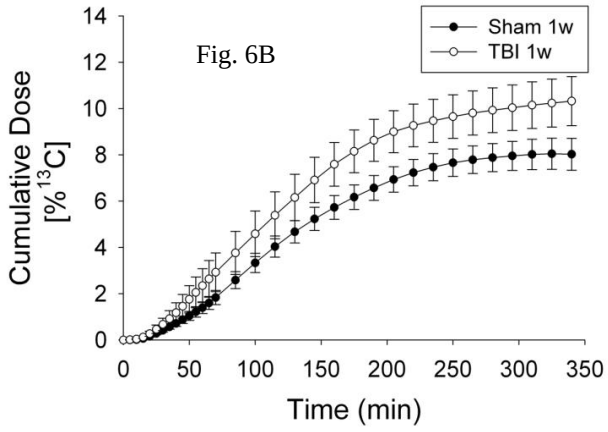

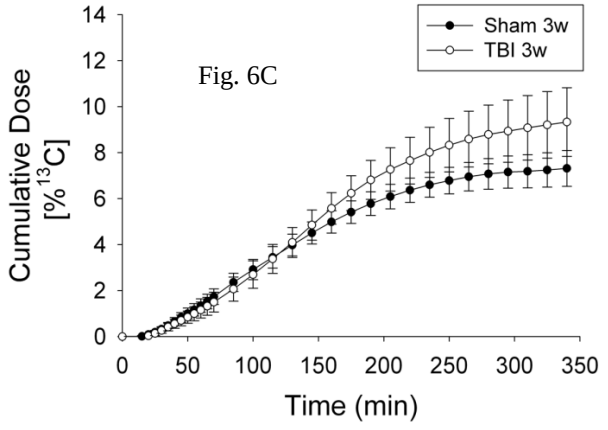

Figure 6. Cumulative dose of ^{13}C respired by FP-TBI and Control groups (shams) at three days (A), one week (B), and three weeks (C) post-FP-TBI or control surgery. Values represent mean ± SEM.

4.3 Immunohistochemistry Failed to Detect the Expression of CRF in the PVN Following FP-TBI

Immunohistochemical detection failed to label CRF-positive neurons or fibers in the PVN of control (Fig. 7A) nor FP-TBI (Fig. 7B) surgery rats. Small CRF-positive fibers were detected in the Median eminence (MEe) following FP-TBI (Fig. 7B).

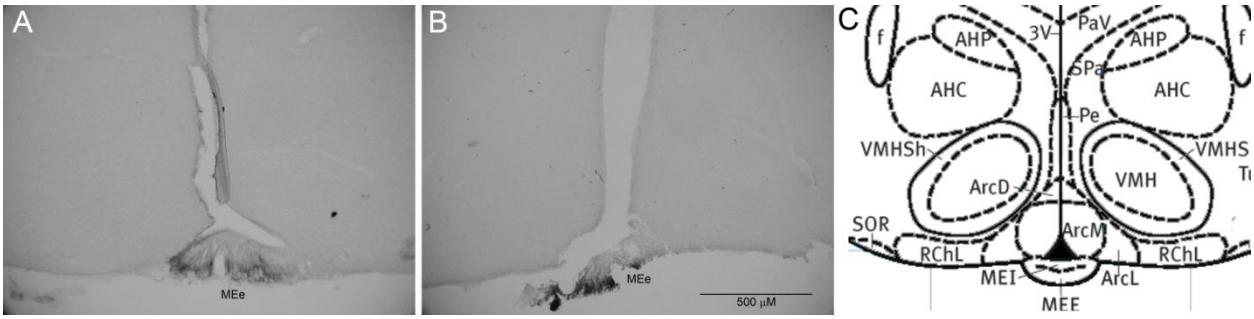

Figure 7. CRF-immunolabeled tissue from Wistar rats at 3 days following control surgery (A) or FP-TBI (B). A representative diagram (C) is shown for comparison. CRF immunohistochemical labeling was confined to the MEe.

4.4 CRF mRNA Is Not Upregulated in the PVN following FP-TBI

At 1 day after FP-TBI (n=8) or control surgery (n=8), CRF mRNA/β-actin ratios demonstrated a non-significant elevation in control than in FP-TBI animals (Fig. 8, $P>0.05$). At 3 days after FP-TBI (n=8) or control surgery (n=8), CRF mRNA/β-actin ratios were similar with only a slight increase in the control group (Fig. 8). The data did not show significant differences at neither 1 day nor 3 days ($P>0.05$).

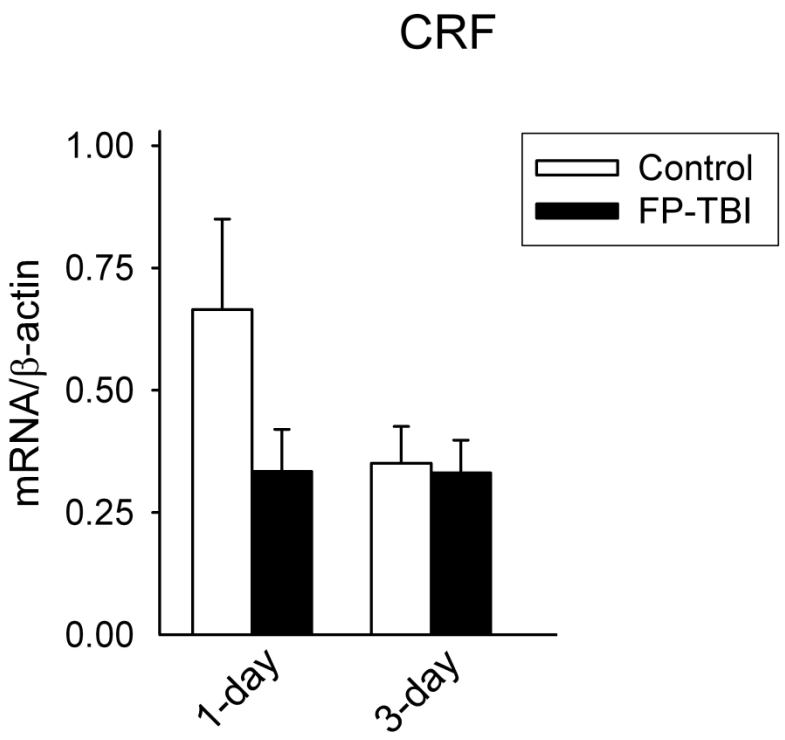

Figure 8. Expression of CRF mRNA was assessed from micropunches of the PVN from FP-TBI and Control rats. Comparisons of CRF mRNA/β-actin ratios in FP-TBI vs. Control animals at 1 day and 3 days were not significantly different.(n=8/group). Values represent mean ± SEM.

4.5 The Effect of Oxytocin on Gastric Motility in FP-TBI and Control Animals

The effect of oxytocin on gastric motility was observed in both FP-TBI (n=19) and control (n=7) animals. In experimental animals, there was no significant effect of PBS on in gastric motility ($P>0.05$) from the PBS injection but there was an effect in gastric motility from the oxytocin injection (Fig. 9). In the representative FP-TBI animal, there was an effect on gastric motility from the oxytocin injection (Fig. 9).

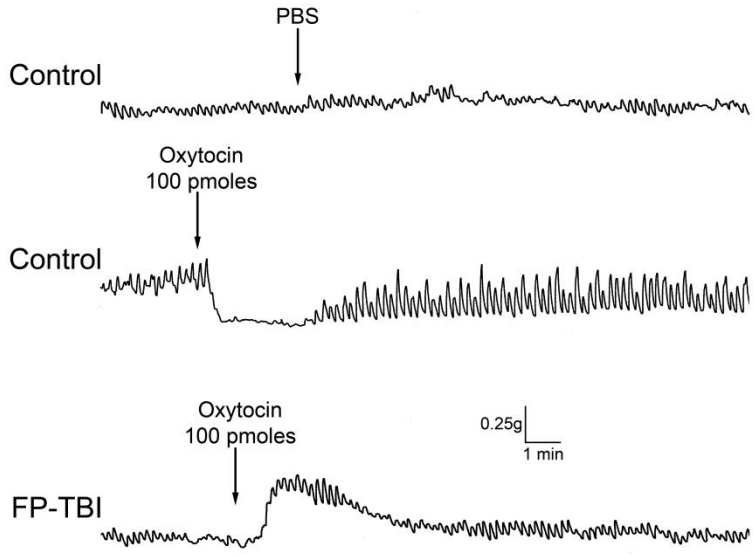

Figure 9. Representative raw motility trace from animals 3 days after FP-TBI or control surgery. Microinjection of PBS into the DVC did not alter motility (upper trace). Inhibition of gastric tone and motility following microinjection of oxytocin in a sham animal (middle trace). Example of an increase in gastric tone following oxytocin injection in a moderate FP-TBI animal (bottom trace).

The changes in gastric tone demonstrated a non-significant increase with the severity of the injury (Fig. 10). Animals receiving a control surgery and animals receiving mild FP-TBI showed comparable reduction in gastric tone while animals receiving moderate FP-TBI showed changes in gastric tone that were higher (Fig. 10). The response to oxytocin was inconsistent within FP-TBI and control groups and among all individual animals.

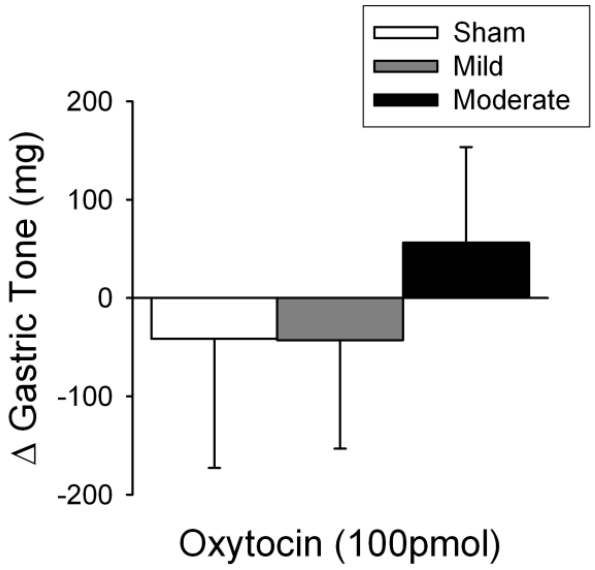

Figure 10. Graphic summary of the change in gastric tone of animals with sham surgery, mild FP-TBI and moderate FP-TBI. Following microinjection of oxytocin, control (sham) and mild FP-TBI animals showed a non-significant decrease in gastric tone relative to baseline. Moderate FP-TBI animals showed a non-significant increase in gastric tone relative to baseline ($P > 0.05$). Values represent mean ± SEM.

Chapter 5: Discussion

In this study, the experimental data indicate that a) our FP-TBI device was consistent, however, the resulting injury wasn't; b) gastric emptying in awake, freely behaving rats was not statistically-significant between control, mild and moderate; c) immunohistochemistry did not reveal any detectable levels of CRF in the hypothalamic PVN, however, CRF expression was demonstrated in the median eminence; d) quantitative RT-PCR reveled a non significant increase in CRF levels in control animals following surgery that did not occur following FP-TBI; and e) moderate FP-TBI non-significantly reversed the effect of oxytocin microinjected into the DVC.

Chronologically, the ^{13}C-octanoic acid breath test was performed first and thus, has the highest mortality percentage at 29.41% of any of the three specific aims. Pilot studies predicted a mortality percentage of 20% so the mortality rates all three of the studies separately as well as the combined mortality rate for all three specific aims were approximately on target.

Mild FP-TBIs were categorized by righting reflex times of five minutes or less and the pressure traces associated with the injuries were very consistent. Our original design presumed a target FP-TBI that would produce righting reflex time from 8-12 minutes. In these experiments, the pressure traces associated with these animals were also extremely consistent, however, a subset of righting reflex times were greater than 12 minutes. These animals were retained for analysis and grouped as moderate FP-TBI for these particular experiments. Fatal FP-TBIs occurred due to CSF leakage out of the nostrils or respiratory failure. The pressure traces associated with these animals were slightly more variable and of higher magnitude. This shows that the injury model was consistent and suggests that the variability of the results may reflect individual anatomical features of each rat.

Preliminary studies that demonstrated a reduction in gastric motility after FP-TBI in anesthetized animals (Holmes, unpublished) led us to hypothesize that gastric emptying in experimental FP-TBI rats will be significantly delayed in comparison to control animals. The value of the 13C breath test is that it is non-invasive and permits multiple tests in an unanesthetized animal (Qualls-Creekmore et al., 2009).

Although our results showed no significant differences in the standard measures of T_{max} or $T_{1/2}$, our different cumulative recovery curves (C_{max}) suggest that there are subtle differences between experimental and sham groups. The higher levels of recovered $^{13}CO_2$ in the FP-TBI animals suggests that a compromised mucosal barrier following FP-TBI could lead to increased permeability or active transport due to barrier dysfunction. A breakdown of intestinal barrier function has been reported following TBI (Bansal et al., 2009; Hang et al., 2003). The resulting bacterial translocation suggests that permeability to a short chain fatty acid (the ^{13}C-octanoic acid substrate used in these experiments) may also occur. An alternative explanation is that active transport of lipids is elevated as a response to TBI. Such a mechanism has been suggested for the upregulation of glucose transport following TBI (Santos et al., 2008).

Previous studies have shown altered hepatic function after TBI (Ziaja et al., 2011; Moinard et al., 2008). A deficit in hepatic function would imply a lower cumulative dose and is in contrast to our current data which shows that FP-TBI animals respire a higher cumulative dose than surgical controls. As this is unlikely according to our data, the differences in the respired cumulative doses of $^{13}CO_2$ as seen in the ^{13}C -non-invasive breath test are not likely due to altered hepatic function.

It is known that CRF is upregulated after stress and that CRF receptors are involved in the inhibition of gastric motility (reviewed in Stengel & Tache, 2010), and while it is commonly difficult, previous studies have shown that levels of CRF are found in the PVN are detectable by immunohistochemistry (Dabrowska et al., 2013). However, these studies universally employ colchicine to inhibit axonal transport and elevate CRF levels without accounting for the global physiological changes associated with colchicine pretreatment. In the present study, a possible explanation as to why immunohistochemistry failed to detect CRF upregulation in the PVN and CRF mRNA was not upregulated in the PVN after FP-TBI is the timing of analysis chosen. We tested for CRF upregulation at 1 day, 3 days and 7 days after FP-TBI. It is possible that by 1 day post-injury CRF levels had peaked and had returned to lower levels of expression. However, in the initial study by Roe (Roe et al., 1998) elevated CRF was detected, by *in situ* techniques, in animals that were sacrificed 3 days following lateral fluid percussion injury. That study overlaps with, and determined, our selected time course.

CRF upregulation is an immediate response to stress. It remains possible that our model of midline FP-TBI (as opposed to lateral FP-TBI) rapidly elicits a CRF response such that collecting and analyzing tissue even 1 day after midline FP-TBI is too late. It is interesting to note that our surgical control animals did demonstrate a non-significant increase in CRF mRNA at 1 day survival. Conversely, our FP-TBI animals displayed no differences between 1 day and 3 days. We speculate that FP-TBI may have actually damaged the hypothalamic PVN neurons to an extent such that CRF levels were negligible. The present experimental design did not permit collection of additional histological sections in order to quantify neuronal death. Silver staining for detecting neural degeneration following FP-TBI has often focused on cortical, hippocampal and brainstem degeneration (Hallam, et al. 2004). Pituitary deficits have been reported

(Greisbach et al., 2011; Taylor et al., 2008) in human and experimental models, although there is no anatomical support for these claims. These studies used lateral FP-TBI and controlled cortical impact models of TBI, respectively, therefore visualizing neurodegeneration fibers throughout the hypothalamus in our model would be a logical future experiment.

Published data have shown that in uninjured animals, microinjection of oxytocin into the DVC inhibits gastric motility and gastric tone (Tache et al., 1990; Holmes et al., 2013). Ongoing studies suggest a reversal in gastric motility after microinjection of oxytocin in the presence of fourth ventricle CRF (Travagli, unpublished). This led us to hypothesize that if, indeed, CRF is present following FP-TBI, oxytocin could be used a pharmacological tool to reverse the inhibition of gastric motility and to indirectly demonstrate a CRF-mediated gastroparesis following FP-TBI. Our data show a non-significant trend in the direction of our hypothesis, but due to such high variability in the anatomical features of each individual rat ($P>0.05$). With more animals and, thus, a reduced variability, these promising results could show significance in the future.

Chapter 6: Conclusion

From the results of this study, it was concluded that the pressure generated by our FP-TBI device was consistent although the subsequent injury was not. It was also demonstrated that gastric emptying in awake, freely-behaving rats was not significantly different between control and FP-TBI groups in these experiments. While CRF expression was demonstrated in the median eminence, immunohistochemistry did not reveal any detectable levels of CRF in the PVN of the hypothalamus. Similarly, quantitative RT-PCR revealed a non-significant increase in CRF levels in control animals following surgery that did not occur following FP-TBI. Finally, it was observed that moderate FP-TBI non-significantly reversed the effect of oxytocin microinjected into the DVC. This result, in light of the unanticipated variability within these experiments, merits further study.

Chapter 7: Future Directions

It is a possibility that barrier dysfunction causes inconsistencies with previously published data. In order to test for barrier dysfunction, Ussing chambers can be used. Parts of the GI tract from FP-TBI and sham animals can be analyzed to observe differences in barrier integrity. Ussing chamber experiments may be found to be more sensitive than motility studies.

Also, it is a good possibility that there is a systemic inflammatory response occurring in these animals that could be causing discrepancies in the results (as reviewed in Anthony et al., 2012). For example, circulating cytokines could be affecting the GI tracts as well as CNS tissue. These studies did not address the role of administering a CRF agonist or antagonist.

While the differential roles of type-1 and type-2 CRF receptors (for example, astressin-type 1, astressin (2)B- type 2), remain unexplored and are a logical avenue for research, dissociating the roles of type 1 vs. type 2 CRF receptors was beyond the scope of these experiments. This route could be explored in order to dissociate the roles of the different types of CRF receptors to decide which would be a good target to study the effect of CRF agonists and antagonists on gastric motility.

Additionally, a recent study hypothesized the role of thrombin production as a mechanism responsible for the post-TBI reduction in gastrointestinal function (Hermann et al., 2009). The authors concluded that PAR-1 activation by thrombin affected gastric motility and inferred that thrombin injections modeled the effects of TBI. While Thrombin release clearly occurs following TBI, these authors over interpreted their model as equivalent to TBI. In order to validate the mechanism that they proposed, TBI studies couple with attention focused upon PAR-1 receptors should be performed.

References

Anthony, D., Couch, Y., Losey, P., & Evans, M. (2012). The systemic response to brain injury and disease. *Brain, Behvaior and Immunity*, 534-540.

Babic, T., Browning, K., & Travagli, R. (2011). Differential organization of excitatory and inhibition synapses within the rat dorsal vagal complex. *American Journal of Physiology. Gastrointestinal and Liver Physiology*, G21-G32.

Babygirija, R., Bulbul, M., Yoshimoto, S., Ludwig, K., & Takahashi, T. (2012). Central and peripheral release of oxytocin following chronic homotypic stress in rats. *Autonomic Neuroscience*, 56-60.

Bansal, V., Costantini, T., Kroll, L., Peterson, C., Loomis, W., Eliceri, B., et al. (2009). Traumatic Brain Injury and Intestinal Dysfunction: Uncovering the Neuro-Enteric Axis. *Journal of Neurotrauma*, 1353-1359.

Bruns, J., & Hauser, W. (2003). The epidemiology of traumatic brain injury: a review. *Epilepsia*, 2-10.

Catania, A., Lonati, C., Sordi, A., & Gatti, S. (2009). Detrimental consequences of brain injury on peripheral cells. *Brain, Behavior and Immunity*, 877-884.

Centers for Disease Control. (2014, March 6). *Injury Prevention & Control: Traumatic Brain Injury*. Retrieved from http://www.cdc.gov/TraumaticBrainInjury/

Cheng, C., & Povlishock, J. (1988). The effect of traumatic brain injury on the visual system: a morphologic characterization of reactive axonal change. *Journal of Neurotrauma*, 47-60.

Clausen, F., & Hillered, L. (2005). Intracranial pressure changes during fluid percussion, controlled cortical impact and weight drop injury in rats. *Acta Neurochirurgica*, 775-780.

Coskun, T., Bozkurt, A., Ozkutlu, U., Kurtel, H., & Yegen, B. (1997). Pathways mediating CRF-induced inhibition of gastric emptying in rats. *Regulatory Peptides*, 113-120.

Dabrowska, J., Hazra, R., Guo, J., Dewitt, S., & Rainnie, D. (2013). Central CRF neurons are not created equal: phenotypic differences in CRF-containing neurons of the rat paraventricular hypothalamus and the bed nucleus of the stria terminalis. *Frontiers in neuroscience*.

Dixon, C. E., Clifton, G. L., Lighthall, J. W., Yaghmai, A. A., & Hayes, R. L. (1991). A controlled cortical impact model of traumatic brain injury in the rat. *Journal of Neuroscience Methods*, 253-262.

Dixon, C., Lyeth, B., Povlishock, J., Findling, R., Hamm, R., Marmarou, A., et al. (1987). A fluid percussion model of experimental brain injury in the rat. *Journal of Neurosurgery*, 110-119.

Ellingson, B., Fijalkowski, R., Pintar, F., Yoganandan, N., & Gennarelli, T. (2005). New mechanism for inducing closed head injury in the rat. *Biomedical sciences instrumentation*, 86-91.

Foda, M., & Marmarou, A. (1994). A new model of diffuse brain injury in rats. Part II: Morphological characterization. *Journal of Neurosurgery*, 301-313.

Gaetz, M. (2004). The neurophysiology of brain injury. *Clinical Neurophysiology*, 4-18.

Geiling, J., Rosen, J. M., & Edwards, R. D. (2012). Medical Costs of War in 2035: Long-Term Care Challenges for Veterans of Iraq and Afghanistan. *Military Medicine*, 1235-1244.

Griesbach, G., Hovda, D., Tio, D., & Taylor, A. (2011). Heightening of the stress response during the first weeks after a mild traumatic brain injury. *Neuroscience*, 147-158.

Hallam, T., Floyd, C., Folkerts, M., Lee, L., Gong, Q., Lyeth, B., et al. (2004). Comparison of behavioral deficits and acute neuronal degeneration in rat lateral fluid percussion and weight-drop brain injury models. *Journal of Neurotrauma*, 521-539.

Hang, C., Shi, J., Li, J., Wu, W., & Win, H. (2003). Alterations of intestinal mucosa structure and barrier function following traumatic brain injury in rats. *World Journal of Gastroenterology*, 2776-2781.

Hermann, G., Van Meter, M., Rood, J., & Rogers, R. (2009). Proteinase-activated receptors in the nucleus of the solitary tract: evidence for glial-neural interactions in autonomic control of the stomach. *The journal of neuroscience: the official journal of the society for neuroscience*, 9292-9300.

Holmes, G., Browning, K., Babic, T., Fortna, S., Coleman, G., & Travagli, R. (2013). Vagal afferent fibres determine the oxytocin-induced modulation of gastric tone. *The Journal of Physiology*, 3081-3100.

Holmes, G., Swartz, E., & McLean, M. (2014). Fabrication and implantation of miniature dual-element strain gages for measuring in vivo gastrointestinal contractions in rodents. *Journal of Visual Experiments*.

Horneman, G., Folkesson, P., Sintonen, H., von Wendt, L., & Emanuelson, I. (2005). Health-related quality of life of adolescents and young adults 10 years after serious traumatic brain injury. *International journal of rehabilitation research*, 245-249.

Krakau, K., Hansson, A., Karlsson, T., de Boussard, C., Tengvar, C., & Borg, J. (2007). Nutritional treatments of patients with severe traumatic brain injury during the first six months after injury. *Nutrition*, 308-317.

Krakau, K., Omne-Ponten, M., Karlsson, T., & Borg, J. (2006). Metabolism and nutrition in patients with moderate and severe traumatic brain injury: A systematic review. *Brain Injury*, 345-367.

Leibson, C., Brown, A., Hall, L. K., Ransom, J., Mandrekar, J., Osler, T., et al. (2012). Medical carecosts associated with traumatic brain injury over the full specturm of disease: a controlled population-based study. *Journal of Neurotrauma*, 2038-2049.

Lewis, M. W., Hermann, G. E., Rogers, R. C., & Travagli, R. A. (2002). In vitro and in vivo analysis of the effects of corticotropin releasing factor on rat dorsal vagal complex. *Journal of Physiology*, 135-146.

Lifshitz, J. (2009). Fluid Percussion Injury Model. In *Animal Models of Acute Neurological Injuries* (pp. 369-380). Totowa, NJ: Humana Press.

Moinard, C., Delpierre, E., Loi, C., Neveux, N., Butel, M., Cynober, L., et al. (2013). An oligomeric diet limits the response to injury in traumatic brain-injured rats. *Journal of Neurotrauma*, 975-980.

Moinard, C., Gupta, S., Besson, V., Morio, B., Marchand-Leroux, C., Chaumeil, J., et al. (2008). Evidence for impairment of hepatic energy homeostasis in head-injured rat. *Journal of Neurotrauma*, 124-129.

Petrov, T., Underwood, B., Braun, B., Alousi, S., & Rafols, J. (2001). Upregulation of iNOS expression and phosphorylation of eIF-2alpha are paralleled by suppression of protein synthesis in rat hypothalamus in a closed head trauma model. *Journal of Neurotrauma*, 799-812.

Pilitsis, J., & Rengachary, S. (2001). Complications of head injury. *Neurological research.*, 227-236.

Qualls-creekmore, E., Tong, M., & Holmes, G. (2010). Time-course of recovery of gastric emptying and motility in rats with experimental spinal cord injury. *Neurogastroenterology & Motility*.

Roasario, E. R., Aqeel, R., Brown, M. A., Sanchez, G., Moore, C., & Patterson, D. (2012). Hypothalamic-Pituitary Dysfunction Following Traumatic Brain Injury Affects

Functional Improvement During Acute Inpatient Rehabilitation. *Journal of Head Trauma Rehabilitation*.

Roe, S., McGowan, E., & Rothwell, N. (1998). Evidence for the involvement of corticotrophin-releasing hormone in the pathogenesis of traumatic brain injury. *The European Journal of Neuroscience*, 553-559.

Santos, A., Goncalves, P., Araujo, J., & Martel, F. (2008). Intestinal permeability to glucose after experimental traumatic brain injury: effect of gadopentetate dimeglumine administration. *Basic & clinical pharmacology & toxicology*.

Schoonjans, R., Van Vlem, B., Van Heddeghem, N., Vandamme, W., Vanholder, R., Lameire, N., et al. (2002). The 13C-octanoic acid breath test: validation of a new noninvasive method of measuring gastric emptying in rats. *Neurogastroenterology and motility: the official journal of the European Gastrointestinal Motility Society*, 287-293.

Stengel, A., & Tache, Y. (2010). Corticotropin-releasing factor signaling and visceral response to stress. *Experimental biology and medicine*, 1168-1178.

Tache, Y., Garrick, T., & Raybould, H. (1990). Central nervous system action of peptides to influence gastrointestinal motor function. *Gastroenterology*, 517-528.

Taylor, A., Rahman, S., Sanders, N., Tio, D., Prolo, P., & Sutton, R. (2008). Injury severity differentially affects short- and long-term neuroendocrine outcomes of traumatic brain injury. *Journal of Neurotrauma*, 311-323.

Teasdale, G., & Jennett, B. (1974). ment of coma and impaired consciousness. A practical scale. *Lancet*, 81-84.

Thompson, H. J., Hoover, R. C., Tkacs, N. C., Saatman, K. E., & McIntosh, T. K. (2005). Development of posttraumatic hyperthermia after traumatic brain injury in rats is associated with increased periventricular inflammation. *Journal of Cerebral Blood Flow & Metabolism*, 163-176.

Travagli, R., Hermann, G., Browning, K., & Rogers, R. (2006). Brainstem circuits regulating gastric function. *Annual review of physiology*, 279-305.

Ulfarsson, T., Arnar, G. G., Rosen, T., Blomstrand, C., Sunnerhagen, K., Lundgren-Nilsson, A., et al. (2013). Pituitary function and functional outcome in adults after severe traumatic brain injury: the long-term perspective. *Journal of Neurotrauma*, 271-280.

Ulrich-Lai, Y. M., & Herman, J. P. (2009). Neural regulation of endocrine and autonomic stress responses. *Nature Reviews Neuroscience*, 397-409.

Walker, K. R., & Tesco, G. (2013). Molecular mechanisms ofcognitive dysfunction following traumatic brain injury. *Frontiers in Aging Neuroscience*.

Wang, X., Dong, Y., Han, X., Qi, X.-Q., Huang, C.-G., & Hou, L.-J. (2013). Nutritional Support for Patients Sustaining Traumatic Brain Injury: A Systematic Review and Meta-Analysis of Prospective Studies. *PLoS One.*

Wang, Y.-B., Liu, J., & Yang, Z.-X. (2011). Effects of intestinal mucosal blood flow and motility on intestinal mucosa. *World Journal of Gastroenterology*, 657-661.

Xiong, Y., Mahmood, A., & Chopp, M. (2013). Animal models of traumatic brain injury. *Nature Reviews Neuroscience*, 128-142.

Zheng, J., Babygirija, R., Bulbul, M., Cerjak, D., Ludwig, K., & Takahashi, T. (2010). Hypothalamic oxytocin mediates adaptation mechanism against chronic stress in rats. *American Journal of Physiology. Gastrointestinal and Liver Physiology.*, G946-G953.

Ziaja, M., Pyla, J., Boczkus, B., Plonka, B., & Plonka, P. (2011). Changes in the nitric oxide level in the rat liver as a response to brain injury. *Nitric Oxide*, 423-430.